Polarization decorrelation in optical fibers with randomly varying elliptical birefringence

T. Wanner

Department of Mathematical Sciences, George Mason University, Fairfax, Virginia 22030

B. S. Marks, C. R. Menyuk, and J. Zweck

Department of Computer Science and Electrical Engineering, University of Maryland, Baltimore County, Baltimore, Maryland 21250

Received May 8, 2003

Polarization decorrelation in single-mode fibers with randomly varying elliptical birefringence is studied. It is found that the effects of ellipticity on the polarization decorrelation length depend on the relative sizes of the beat length and the autocorrelation length of the birefringence fluctuations in the fiber. However, the evolution of the differential group delay remains unaffected by ellipticity. © 2003 Optical Society of America

OCIS code: 260.1440.

Polarization mode dispersion is an important phenomenon in modern long-distance communication fibers, since it induces signal distortion along the length of a communication link. The physical origin of polarization mode dispersion lies in the random, rapidly varying birefringence present in any optical fiber, which leads to pulse spreading. This random birefringence is characterized by two material properties of the fiber: the average beat length, L_B, and the autocorrelation length, h_{fiber}. Both of these parameters depend on environmental conditions and cabling, and it is often difficult to relate them directly to phenomena that affect the transmission of data signals through the system, such as the randomization of the signal's polarization state on the Poincaré sphere and the differential group delay (DGD).

Previous studies of these phenomena have made one of two simplifying assumptions, representing two limiting cases: (1) Fibers are only linearly birefringent, arguing that the ellipticity is small enough to be negligible in actual fibers,[1,2] or (2) all birefringences are equally probable, leading to isotropic diffusion of the signal's polarization state on the Poincaré sphere.[3] In both cases, the DGD has the same behavior, but the randomization of the signal's polarization state is different. The second birefringence model of Wai and Menyuk[1,2] considers only linear birefringence, and it is the only model that is consistent with experimental evidence.[4] This model was used to calculate the evolution of the DGD as a function of propagation distance. It is known, however, that fibers have a small elliptical birefringence caused by twisting the fiber.[5] In this Letter we use a stochastic model to systematically study the effect of this residual ellipticity. We show that, although the DGD is not affected by the introduction of ellipticity, the randomization of the signal's polarization state on the Poincaré sphere is affected.

The key material parameters of the fiber that are necessary to understand these effects are the average beat length, L_B, and the autocorrelation length of the birefringence fluctuations in the fiber, h_{fiber}, which were mentioned above. The extent to which the polarization state of a signal is randomized on the Poincaré sphere as a result of birefringence fluctuations is described by additional parameters. In this Letter we concentrate on one such parameter, the polarization decorrelation length, h_E, which is the length scale over which the electric field loses memory of its initial distribution between the local polarization eigenstates and can be treated as random. In certain special cases it is possible to derive analytical formulas relating h_E to L_B and h_{fiber}. These cases include the diffusion limit $h_{\mathrm{fiber}} \ll L_B$ studied by Ueda and Kath[6] for linearly birefringent fibers and the weak-coupling limit $L_B \ll h_{\mathrm{fiber}}$ studied by Poole[7] for isotropically birefringent fibers. Since neither of these limits necessarily holds in optical fibers, Wai and Menyuk[1] used simulations to determine the dependence of h_E on h_{fiber} and L_B for linearly birefringent fibers. We extend their results to the case of elliptical birefringence.

After removal of the variation common to both components of the electrical field vector of a signal, $\mathbf{A}$, the z dependence of $\mathbf{A}$ is governed by the equation

$$\frac{\mathrm{d}\mathbf{A}}{\mathrm{d}z} = i\begin{bmatrix} x_1 & x_2 + ix_3 \\ x_2 - ix_3 & -x_1 \end{bmatrix}\mathbf{A}\,. \tag{1}$$

The parameters x_1, x_2, and x_3 describe the evolution of the local birefringence, with x_1 and x_2 parameterizing linear birefringence and x_3 parameterizing elliptical birefringence. Our dynamical model for x_1, x_2, and x_3 is an extension of the second model of Wai and Menyuk.[1,2] In their model, $x_3 = 0$, and the evolution of x_1 and x_2 is described by independent Langevin processes:

$$\mathrm{d}x_k/\mathrm{d}z = -\alpha x_k + \sigma g_k(z)\,, \qquad k = 1, 2\,, \tag{2}$$

where g_1 and g_2 are independent white-noise processes with the properties

0146-9592/03/191799-03$15.00/0

$$E[g_k(z)] = 0\,, \qquad E[g_k(z)g_k(z+u)] = \delta(u)\,, \qquad k = 1, 2\,, \quad (3)$$

with $\delta(u)$ being the Dirac distribution. We extend this model by adding an independent Langevin equation for the third parameter x_3, namely,

$$\mathrm{d}x_3/\mathrm{d}z = -\alpha x_3 + \tau g_3(z)\,, \quad (4)$$

where g_3 denotes another white noise process satisfying Eqs. (3), independent of g_1 and g_2. The ratio of the noise intensities, τ/σ, is a measure of the amount of ellipticity present in our model. When $\tau/\sigma = 0$ we recover the second Wai and Menyuk model of linear birefringence, and when $\tau/\sigma = 1$ the birefringence vector varies isotropically. The fiber characteristics h_{fiber} and L_B can easily be expressed in terms of the parameters in Eqs. (2) and (4). One can show that $h_{\mathrm{fiber}} = 1/\alpha$ and $L_B = \pi[2\alpha/(2\sigma^2 + \tau^2)]^{1/2}$.

To determine the dependence of h_E on the ratio h_{fiber}/L_B, we have to simulate the evolution of the electric field. Rather than using Eq. (1), we switch to the Poincaré sphere representation. In this form, the evolution of the Stokes vector of the signal is given by

$$\mathrm{d}\mathbf{S}/\mathrm{d}z = \mathbf{W}(z, \omega) \times \mathbf{S}\,, \quad (5)$$

where $\mathbf{W}(z, \omega) = (2x_1, 2x_2, 2x_3)^t$ is the local birefringence vector. Instead of using the fixed coordinate frame as in Eq. (5), we consider three different coordinate frames. Coordinate frame A is obtained by a z-dependent rotation about the S_3 axis that transforms the local birefringence vector $\mathbf{W}(z, \omega)$ into the S_1–S_3 plane. Coordinate frame B is obtained by a z-dependent rotation about the S_3 axis chosen so that the initial birefringence vector $\mathbf{W}(0, \omega)$ is in the S_1–S_3 plane. Finally, coordinate frame C is obtained by the same rotation about the S_3 axis as in frame A, followed by a rotation about the S_2 axis that transforms the local birefringence vector $\mathbf{W}(z, \omega)$ so that it is in the direction of the vector $(1, 0, 0)^t$. Notice that coordinate frames A and B correspond to the ones used in Refs. 1 and 2. Coordinate frames B and C represent two limiting situations. In frame C we consider only the local motion of the signal's Stokes parameters relative to the birefringence vector, whereas in frame B the Stokes parameters move relative to a fixed frame. Consequently, we expect the polarization decorrelation length h_E in any other reference frame to be between these two limits. However, in frame A the amount of ellipticity is preserved by the rotation, and therefore this frame is physically more reasonable than frame C.

We define the polarization decorrelation length h_E as the distance over which the ensemble average of S_1, $\langle S_1(z)\rangle$, drops to $1/e$ of its initial value. For each simulation, we define the initial Stokes vector to be pointing in the direction of the initial local birefringence vector. In the case $\tau/\sigma = 0$, corresponding to linear birefringence, $\langle S_1(0)\rangle = 1$. However, for coordinate frames A and B the ensemble average $\langle S_1(0)\rangle$ decreases from a value of 1 when $\tau/\sigma = 0$ to a value of $\pi/4$ when $\tau/\sigma = 1$. We solved the underlying stochastic differential equation by use of a strong Taylor scheme of the order of 1.5.[8] For Figs. 1 and 2, our ensemble size is 30,000, and for Fig. 3 we used 60,000 realizations.

We are interested in the behavior of the polarization decorrelation length as a function of h_{fiber}/L_B. Figure 1 shows the results of our simulations for various values of the noise intensity ratio, τ/σ. We find that the polarization decorrelation length is almost identical when measured in the two local frames, A and C. Moreover, for both frames, introducing ellipticity increases the computed values of h_E, but only slightly, by ~8%. The resulting behavior of h_E as a function of

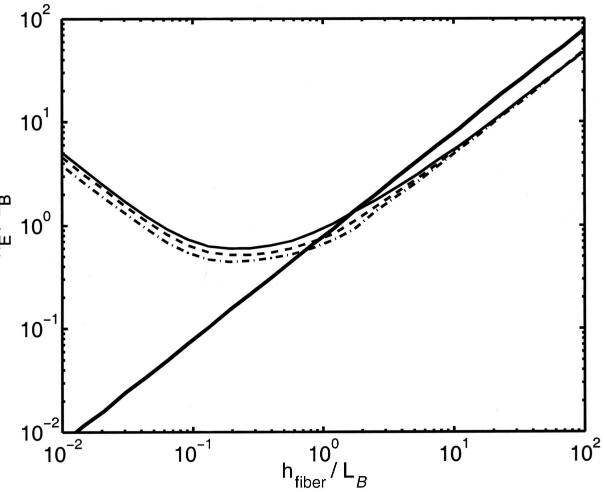

Fig. 1. Polarization decorrelation length versus h_{fiber}/L_B. The thick solid line represents the results for local coordinate frame A and $\tau/\sigma = 0$; on the scale of the figure, the results for other values of τ/σ or for coordinate frame C are indistinguishable. The remaining three curves show the results for frame B, with τ/σ ratios 0, 0.5, and 1 represented by the thin solid, dashed, and dashed–dotted curves, respectively.

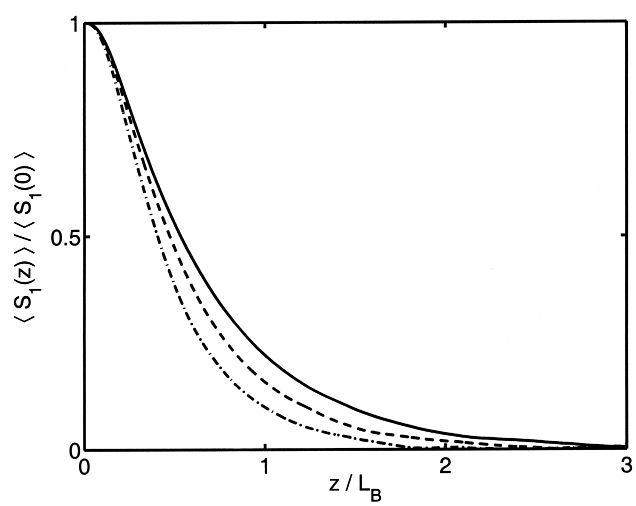

Fig. 2. Graphs of $\langle S_1(z)\rangle/\langle S_1(0)\rangle$ versus distance z for $h_{\mathrm{fiber}}/L_B = 0.1$ when measured in coordinate frame B. The τ/σ ratios 0, 0.5, and 1 are represented by the solid, dashed, and dashed–dotted curves, respectively.

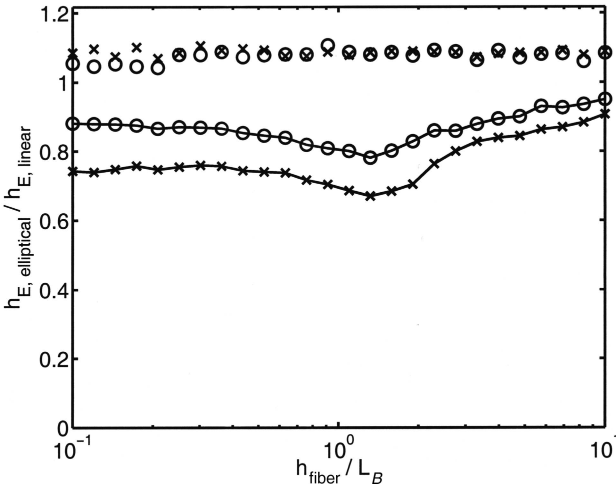

Fig. 3. Polarization decorrelation lengths with ellipticity versus h_{fiber}/L_B, relative to the corresponding lengths without ellipticity. The circles and the curve with circles show the results for coordinate frames A and B, respectively, when $\tau/\sigma = 0.5$. The corresponding results for the isotropic case $\tau/\sigma = 1$ are shown by crosses and the curve with crosses, respectively.

h_{fiber}/L_B is represented by the thick solid line in Fig. 1. On the scale used in Fig. 1, the increased ellipticity leads to no visually detectable change in the graph. These simulations also show that, with respect to either local coordinate system, the polarization decorrelation length is proportional to the fiber decorrelation length, h_{fiber}, independent of the ratio τ/σ. This result has important implications for the evolution of the DGD, as discussed shortly.

As one can see in Fig. 1, the situation is different in the fixed coordinate frame, B. In this case an increase in ellipticity can lead to a noticeable decrease in the polarization decorrelation length. This decrease can be observed only if the ratio h_{fiber}/L_B is less than 10, as is evident from the three convex curves in Fig. 1. These curves correspond to ratios τ/σ of 0, 0.5, and 1. Notice, however, that the curves retain their general dependence on h_{fiber}/L_B. As a typical example of the observed decrease in the polarization decorrelation length, in Fig. 2 we show the evolution of $\langle S_1(z)\rangle/\langle S_1(0)\rangle$ along the fiber for $h_{\text{fiber}}/L_B = 0.1$ and for the ratios of τ/σ given above. In this case, the polarization decorrelation length for $\tau/\sigma = 1$ is ~25% lower than for $\tau/\sigma = 0$. Quantitative information on the relative changes in the polarization decorrelation length is given in Fig. 3 for values of h_{fiber}/L_B from 0.1 to 10. For local frame A, if we increase τ/σ from 0 to 1, we observe a uniform increase in h_E, independent of h_{fiber}/L_B, whereas for fixed frame B, as we increase τ/σ, h_E decreases by an amount that depends on h_{fiber}/L_B. The largest decrease in h_E is by ~35% and occurs when $h_{\text{fiber}} \approx L_B$.

Next we discuss the evolution of the DGD, which is given by the ensemble average $\langle {\tau_d}^2\rangle = \langle {\Omega_1}^2 + {\Omega_2}^2 + {\Omega_3}^2\rangle$, where $\mathbf{\Omega} = (\Omega_1, \Omega_2, \Omega_3)^t$ denotes the polarization dispersion vector. Its evolution is governed by

$$\frac{\mathrm{d}\mathbf{\Omega}}{\mathrm{d}z} = \frac{\partial \mathbf{W}}{\partial \omega} + \mathbf{W} \times \mathbf{\Omega}\,. \tag{6}$$

As in Refs. 2 and 3, we assume that the orientation of the birefringence axis is a function of z alone and that the frequency variation of the birefringence strength is separable from its z variation, i.e., $\mathbf{W}(z, \omega) = k(\omega) \cdot \widetilde{\mathbf{W}}(z)$. We also suppose that $k(\omega)$ is a deterministic function of frequency. Then it is possible to solve the stochastic differential equation given by Eqs. (2), (4), and (6) exactly, leading to the expression

$$\langle {\tau_d}^2\rangle = 2{h_{\text{fiber}}}^2\langle \Delta'^2\rangle[\exp(-z/h_{\text{fiber}}) + z/h_{\text{fiber}} - 1], \tag{7}$$

where $\langle \Delta^2\rangle$ denotes the asymptotic value of the birefringence strength.[2] Notice that Eq. (7) holds regardless of the specific ratio τ/σ, consistent with Refs. 2 and 3. Thus, if all one cares about is the DGD, then the simplifying assumption that all birefringences are equally probable yields the correct answer.

In conclusion, we have described the dependence of the polarization decorrelation length, h_E, on the amount of ellipticity present in an optical fiber. These results demonstrate in particular that Eq. (7) remains valid regardless of the strength of ellipticity and that in a local coordinate frame the polarization decorrelation length, h_E, is proportional to the fiber autocorrelation length, h_{fiber}. A small ellipticity does not significantly affect results that are predicted by a model that assumes that fibers are linearly birefringent.

T. Wanner's e-mail address is wanner@math.gmu.edu

References

1. P. K. A. Wai and C. R. Menyuk, Opt. Lett. **19,** 1517 (1994).
2. P. K. A. Wai and C. R. Menyuk, J. Lightwave Technol. **14,** 148 (1996).
3. N. Gisin, Opt. Commun. **86,** 371 (1991).
4. A. Galtarossa, L. Palmieri, M. Schiano, and T. Tambosso, Opt. Lett. **25,** 1322 (2000).
5. R. Ulrich and A. Simon, Appl. Opt. **18,** 2241 (1979).
6. T. Ueda and W. L. Kath, Physica D **55,** 166 (1992).
7. C. D. Poole, Opt. Lett. **13,** 687 (1988).
8. P. E. Kloeden and E. Platen, *Numerical Solution of Stochastic Differential Equations* (Springer, New York, 1992).